

EXTENDED REPORT

A CD4 T cell gene signature for early rheumatoid arthritis implicates interleukin 6-mediated STAT3 signalling, particularly in anti-citrullinated peptide antibody-negative disease

Arthur G Pratt,^{1,2} Daniel C Swan,³ Sarah Richardson,¹ Gillian Wilson,² Catharien M U Hilkens,¹ David A Young,¹ John D Isaacs^{1,2}

► Additional data are published online only. To view these files please visit the journal online (<http://ard.bmj.com/content/early/recent>).

¹Institute of Cellular Medicine (Musculoskeletal Research Group), Newcastle University, Newcastle upon Tyne, UK

²Musculoskeletal Directorate, Newcastle upon Tyne Hospitals NHS Trust, Newcastle upon Tyne, UK

³Institute of Cell and Molecular Biology (Bioinformatics Support Unit), Newcastle University, Newcastle upon Tyne, UK

Correspondence to

Professor John D Isaacs, Newcastle University, Institute of Cellular Medicine (Musculoskeletal Research Group), Newcastle upon Tyne NE2 4HH, UK; j.d.isaacs@ncl.ac.uk

Accepted 23 February 2012

ABSTRACT

Objective We sought clinically relevant predictive biomarkers present in CD4 T-cells, or in serum, that identified those patients with undifferentiated arthritis (UA) who subsequently develop rheumatoid arthritis (RA).

Methods Total RNA was isolated from highly purified peripheral blood CD4 T cells of 173 early arthritis clinic patients. Paired serum samples were also stored.

Microarray analysis of RNA samples was performed and differential transcript expression among 111 'training cohort' patients confirmed using real-time quantitative PCR. Machine learning approaches tested the utility of a classification model among an independent validation cohort presenting with UA (62 patients). Cytokine measurements were performed using a highly sensitive electrochemiluminescence detection system.

Results A 12-gene transcriptional 'signature' identified RA patients in the training cohort and predicted the subsequent development of RA among UA patients in the validation cohort (sensitivity 68%, specificity 70%). STAT3-inducible genes were over-represented in the signature, particularly in anti-citrullinated peptide antibody-negative disease, providing a risk metric of similar predictive value to the Leiden score in seronegative UA (sensitivity 85%, specificity 75%). Baseline levels of serum interleukin 6 (IL-6) (which signals via STAT3) were highest in anti-citrullinated peptide antibodies-negative RA and distinguished this subgroup from non-RA inflammatory synovitis (corrected $p < 0.05$). Paired serum IL-6 measurements correlated strongly with STAT3-inducible gene expression.

Conclusion The authors have identified IL-6-mediated STAT-3 signalling in CD4 T cells during the earliest clinical phase of RA, which is most prominent in seronegative disease. While highlighting potential biomarker(s) for early RA, the role of this pathway in disease pathogenesis awaits clarification.

The importance of prompt disease-modifying therapy in early rheumatoid arthritis (RA) is now established.^{1,2} Yet about 40% of patients with new-onset inflammatory arthritis present with disease that is unclassifiable at inception, having a so-called undifferentiated arthritis (UA).³ Timely intervention for the subset of these UA patients who subsequently develop RA therefore remains problematic. The issue is highlighted by the publication of updated

RA classification criteria⁴ and a validated 'prediction rule' that foretells risk of UA progression to RA.⁵ Such approaches rely heavily on autoantibody status, emphasising the specificity of circulating anti-citrullinated peptide antibodies (ACPA) for RA.⁶ Consequently, the diagnosis of ACPA-negative RA remains challenging in the early arthritis clinic (EAC), being frequently delayed despite application of the prediction rule.⁷

The potential for the whole-genome transcription profiling to yield clinically relevant prognostic 'gene signatures' in autoimmune disease has been demonstrated.^{8,9} Applying a similar, prospective approach to the discovery of predictive biomarkers in UA should complement existing diagnostic algorithms, while providing new insights into disease pathogenesis.¹⁰ However, the use of peripheral blood (PB) mononuclear cells for transcriptional analysis may result in data that are biased by relative subset abundance.¹¹ To address this, protocols for rapid ex vivo positive selection of cell subsets for the purpose of transcription profiling have been validated.¹² Although no single cell-type is exclusively implicated in RA, many of its established and emerging genetic associations implicate the CD4 T cell.¹³ We therefore hypothesised that the PB CD4 T-cell transcriptome would provide a useful substrate for both biomarker discovery and a pathophysiological understanding of RA induction.

MATERIALS AND METHODS

A complete description of experimental and bioinformatics approaches are given in the online supplementary text.

Patients

Patients with recent onset arthritis, naïve to disease-modifying anti-rheumatic drugs and corticosteroids, were recruited between September 2006 and December 2008. An initial working clinical diagnosis was updated by the consulting rheumatologist at consecutive clinic visits for the duration of the study—median 28 months and >12 months in all cases. RA was diagnosed only where 1987 American College of Rheumatology classification criteria¹⁴ were fulfilled; UA was defined as a 'suspected inflammatory arthritis where RA remained a possibility, but where established classification criteria for any rheumatological condition remained



This paper is freely available online under the BMJ Journals unlocked scheme, see <http://ard.bmj.com/info/unlocked.dtl>

Table 1 Clinical characteristics of the rheumatoid arthritis (RA) and non-RA comparator groups used to generate list of differentially expressed genes, which together comprise a training cohort for machine-learning (total n=111) and the independent undifferentiated arthritis (UA) validation cohort (n=62)

	Training cohort			Test cohort
	RA (n=47)	Non-RA (n=64)	p*	UA† (n=62)
Age (years; mean, SD range)	60 (46–74)	48 (34–62)	0.01	52 (37–67)
% Female	65	61	NS	77
% White Caucasian	96	92	NS	90
Symptom duration (weeks; median, IQR)	12 (8–24)	21 (10.5–52)	0.026	14 (12–26)
Tender joint count (median, IQR)	10 (4–15)	7 (2–14)	NS	8 (3–16.5)
Swollen joint count (median, IQR)	6 (2–10)	0 (0–2)	<0.001	1 (0–3)
Morning stiffness (hours; median, IQR)	1 (0.75–2)	0.75 (0.1–2)	0.007	1 (0.5–2)
ESR (s; median, IQR)	56 (30–78)	24 (14–52)	<0.001	30 (18–60)
CRP (g/l; median, IQR)	17 (9–62)	5 (2.5–19)	<0.001	8.5 (0–17)
ACPA+ (number; per cent)	29 (62)	0 (0)	<0.001	13 (21)
RF+ (number; per cent)	36 (77)	3 (6)	<0.001	20 (32)
DAS28 (median)	5.37	NA	–	
Leiden prediction score (median, IQR)	NA	NA	–	6.4 (5–7.6)
Outcome diagnoses (number, per cent)				
RA	47 (100)	0 (0)	–	25 (40)
Seronegative spondyloarthropathy	–	22 (34)	–	8 (13)
Self-limiting inflammatory	–	12 (19)	–	9 (15)
Other inflammatory	–	3 (5)	–	2 (3)
OA/non-inflammatory	–	27 (42)	–	18 (29)

Values are mean (1 SD range), median (IQR) or % for normally distributed, skewed or dichotomous data, respectively.

* Statistical tests for significant difference between RA and non-RA groups; t-test, Mann–Whitney U or Fisher's exact test for normally distributed, skewed or dichotomous data, respectively.

† Demographic, clinical and serological parameters are given for UA–RA and UA–non-RA subgroups in online supplementary table S2.

ACPA, anti-citrullinated peptide antibodies; CRP, C reactive protein; DAS28, disease activity score (incorporating 28-swollen/tender joint counts);

ESR, erythrocyte sedimentation rate; NS, not significant; OA, osteoarthritis; RA, rheumatoid arthritis; RF, rheumatoid factor; UA, undifferentiated arthritis.

unmet' (see online supplementary text and supplementary table S1). Individuals whose arthritis remained undifferentiated at the end of the study were excluded. Patients gave written informed consent before inclusion into the study, which was approved by the local regional ethics committee.

CD4 T-cell RNA processing and array analysis

Whole blood drawn between 13:00 and 16:30 was stored at room temperature for ≤4 h before processing. After monocyte depletion by immuno-rosetting, an automated magnetic bead-based positive selection protocol was used to isolate CD4 cells (Stemcell Technologies, Vancouver, Canada). Using this approach, a median CD4 T-cell purity of 98.9% was achieved (range 95–99.7%), which was determined using flow cytometry (see online supplementary figure S1). Total CD4 T-cell RNA was immediately extracted, then quality controlled using an Agilent 2100 Bioanalyzer (Agilent, Santa Clara, California, USA). The median RNA integrity number¹⁵ of samples used was 9.4. cRNA generated from 250 ng total RNA (Illumina TotalPrep RNA Amplification Kit) was hybridised to the Illumina Whole Genome 6v3 BeadChip (Illumina, San Diego, California, USA), representing 48 804 known genes and expressed sequence tags. Array data were processed using Illumina BeadStudio software, then it was normalised, batch corrected,¹⁶ filtered and quality controlled as described (online supplementary text and figure S2).

To define differential expression a fold-change cut-off of 1.2 between comparator groups was combined with a significance level cut-off of $p < 0.05$ (Welch's *t*-test), corrected for multiple testing using the false-discovery-rate method of Benjamini *et al.*¹⁷ Genes thereby identified were used to train a support vector machine (SVM) classification model based on known outcomes among a 'training' sample set.¹⁸ The model's accuracy as a prediction tool was then assessed among an independent

'validation' sample set. To obtain larger lists of differentially expressed genes for biological pathway analysis, significance thresholds were relaxed through the omission of multiple-test-correction and Ingenuity Pathways Analysis software (Ingenuity Systems, Redwood City, California, USA) was then employed.

Serum cytokine measurement

Between 13:00 and 16:30, baseline serum was drawn and frozen at -80°C until use. Serum interleukin 6 (IL-6), soluble IL-6 receptor (sIL6R), tumour necrosis factor α (TNF α), leptin and granulocyte colony stimulating factor concentrations were measured using a highly sensitive electrochemiluminescence immunosorbance detection system (Meso Scale Discovery, Gaithersburg, Maryland, USA), assays having been validated as outlined (online supplementary text and figure S3).

Quantitative real-time PCR

CD4 T cell total RNA samples were reverse transcribed using superscript II reverse transcriptase and random hexamers, according to the manufacturer's instructions (Invitrogen, Carlsbad, California, USA). Real-time PCR reactions were performed as part of a custom-made TaqMan Low Density Array (7900HT real-time PCR system, Applied Biosystems, Foster City, California, USA). Raw data were normalised and expressed relative to the housekeeping gene β -actin as $2^{-\Delta\text{Ct}}$ values.¹⁹

General statistics

Parametric and non-parametric analyses of variance, Mann–Whitney U tests, Pearson's correlation coefficients, intra-class correlations, multivariate analyses and the construction of receiver operator characteristic (ROC) curves were performed, as described, using SPSS version.15.0 (SPSS, Chicago, Illinois, USA). The derivation of Leiden prediction rules⁵ and transcrip-

Table 2 Fold-change and significance level for genes differentially expressed at inception among peripheral blood CD4 T cells between early arthritis clinic patients with inception diagnoses of RA and non-RA (confirmed at ≥ 1 year; median 28 months follow-up). The official gene symbol and RefSeq accession number are given as identifiers. Listed STAT3-regulated genes are italicised. 12 genes included in statistically most robust 'RA signature' appear in boldface, and additional STAT3-regulated genes referred to in text are also provided

Gene (Accn. No.) <i>12-Genes RA Signature:</i>	Microarray data (47 RA vs 64 non-RA)			qRT-PCR data (32 RA vs 41 non-RA*)	
	FC	Uncorr. p†	Corr. p†	FC	p‡
<i>BCL3</i> (NM_005178)	1.59	2.6×10^{-5}	0.03	2.15	0.005
<i>SOCS3</i> (NM_003955)	1.55	3.4×10^{-6}	0.03	1.83	0.002
<i>PIM1</i> (NM_002648)	1.52	6.8×10^{-6}	0.03	1.67	0.001
<i>SBNO2</i> (NM_014963)	1.47	1.2×10^{-5}	0.03	1.13	0.158
<i>LDHA</i> (NM_005566)	1.23	3.8×10^{-5}	0.04	1.25	0.003
<i>CMAH</i> (NR_002174)	1.2	1.7×10^{-5}	0.03	1.40	0.003
<i>NOG</i> (NM_005450)	-1.32	3.1×10^{-5}	0.03	-1.59	0.004
<i>PDCD1</i> (NM_005018)	1.42	1.0×10^{-5}	0.03	ND	ND
<i>IGFL2</i> (NM_001002915)	1.31	1.1×10^{-7}	0.002	ND	ND
<i>LOC731186</i> (XM_001128760)	1.28	2.3×10^{-5}	0.03	ND	ND
<i>MUC1</i> (NM_001044391)	1.26	2.0×10^{-5}	0.03	ND	ND
<i>GPRIN3</i> (CR743148)§	1.32	2.1×10^{-4}	0.049	ND	ND
<i>Additional STAT3-regulated:</i>					
<i>ID3</i> (NM_002167)	-1.3	5.2×10^{-4}	0.16	ND	ND
<i>MYC</i> (NM_002467)	1.2	0.04	0.75	1.29	0.01

*Baseline characteristics of Quantitative real-time PCR validation sub-cohort are similar to those of the training cohort overall (table 1) and are given in the online supplementary table S4.

†Calculations based on normalised expression values of array data; Welch's t-test, raw and multiple-test-corrected p values given (see methods).

‡Calculations based on expression data normalised to the house-keeping gene β -actin ($2^{-\Delta\Delta C_t}$); Mann-Whitney U test (see methods).

§Transcript *CR743148* (Illumina Probe ID 6370082) has been retired from NCBI, but the expressed sequence tag corresponds to splice variant(s) within the *GPRIN3* gene (chromosome 4.90).

FC, linearised fold-change expression in RA relative to non-RA (ie, negative values represent genes downregulated in RA relative to non-RA by v-fold); ND, not done; RA, rheumatoid arthritis.

tional 'risk metrics' for ACPA-negative RA is outlined in the online supplementary text.

RESULTS

Patient groups

A total of 173 patient samples were retrospectively selected for microarray analysis. One hundred and eleven of these originated from patients assigned definitive diagnoses at inception, confirmed at a median 28 months follow-up (minimum 1 year); an RA versus non-RA discriminatory 'signature' was derived from this 'training cohort' alone. The remaining 62 samples, all representing UA patients, formed an independent 'validation cohort' for testing the utility of the 'signature' according to diagnostic outcomes as they evolved during the same follow-up period. As expected, the characteristics of the UA cohort (age, acute phase response, joint counts, etc.) fell between the equivalent measurements in the RA and control sample sets within the training cohort (table 1). For subsequent pathway analysis, all 173 samples were pooled before being divided into four categories based on diagnostic outcome at the end of the study (see online supplementary table S2).

RA transcription 'signature' most accurate in ACPA-negative UA

Using a significance threshold robust to multiple test correction (false-discovery-rate $p < 0.05$),¹⁷ 12 genes were shown to be differentially expressed (>1.2 -fold) in PB CD4 T cells between 47 'training cohort' EAC patients with a confirmed diagnosis of RA, and 64 who could be assigned non-RA diagnoses (table 2).

An extended list, obtainable by omitting multiple-test correction, appears as online supplementary gene-list 1. Supervised hierarchical cluster analysis of the resultant dataset (111 samples, 12 genes), demonstrated a clear tendency for EAC patients diagnosed with RA to cluster together based on this transcription profile (figure 1A). Quantitative real-time PCR (qRT-PCR) was used to analyse expression of seven of the differentially expressed genes in a subset of 73 samples (for baseline characteristics of this subset, see online supplementary table S4). Despite the reduced power to detect change in this smaller dataset, robust differential expression was confirmed for six of the seven genes (table 2).

To derive a metric denoting risk of progression to RA, the sum of normalised expression values for the 12-gene RA 'signature' was calculated for each individual in the training cohort (see online supplementary text). A ROC curve was constructed for this risk metric, the area under which (0.85; SEM=0.04) suggested promising discriminatory utility (figure 1B). A SVM based on the training cohort dataset was then applied to classify members of the validation cohort, correctly identifying UA patients who developed RA with a sensitivity, specificity, positive and negative likelihood ratio (0.68, 95% CI 0.48 to 0.83); 0.70, 95% CI 0.60 to 0.87); 2.2, 95% CI 1.2 to 3.8) and 0.4 95% CI 0.2 to 0.8), respectively. However, we observed that of the 13 ACPA-positive UA patients, 12 progressed to RA, indicating that autoantibody status alone was a more sensitive predictor of RA in this subset. By contrast, when applied exclusively to the ACPA-negative subset of the UA validation cohort ($n=49$), the SVM classification model provided a sensitivity of 0.85 (95% CI 0.58 to 0.96) and a specificity of 0.75 (0.59-0.86) for progression to RA, thereby performing best in this diagnostically most challenging patient group. Hierarchical clustering of the ACPA-negative UA samples based on their 12-gene RA 'signature' expression profiles further illustrates molecular similarities within the ACPA-negative RA outcome group (figure 1C).

Gene signature adds value to existing tools in diagnosing ACPA-negative UA

Next, we tested the value of our 12-gene signature in comparison with the existing 'Leiden prediction rule' as a predictor of RA among UA patients.⁵ While the discriminatory utility achieved by the prediction rule in our UA cohort was comparable with that previously reported ($n=62$; AU ROC curve=0.86; SEM=0.05, data not shown), its performance diminished among the ACPA-negative sub-cohort ($n=49$; AU ROC curve=0.74; SEM=0.08; figure 1D). Employing a 12-gene risk metric, as described above, equivalent discriminatory utility was found in this sub-cohort (AU ROC curve=0.78; SEM=0.08, data not shown). However, by deriving a modified risk metric, which combined all features of the Leiden prediction rule with our 12-gene risk metric (see online supplementary text and table S5), and applying it to the independent ACPA-negative UA cohort, we could improve the utility of the prediction rule for seronegative UA patients (AU ROC=0.84; SEM=0.06; figure 1D).

STAT3 transcription profile is most prominent in ACPA-negative RA

All 173 patients studied were now grouped into four categories based on outcome diagnosis alone: ACPA-positive RA, ACPA-negative RA, inflammatory non-RA controls and osteoarthritis(OA); their demographic and clinical characteristics are presented for comparison (online supplementary table

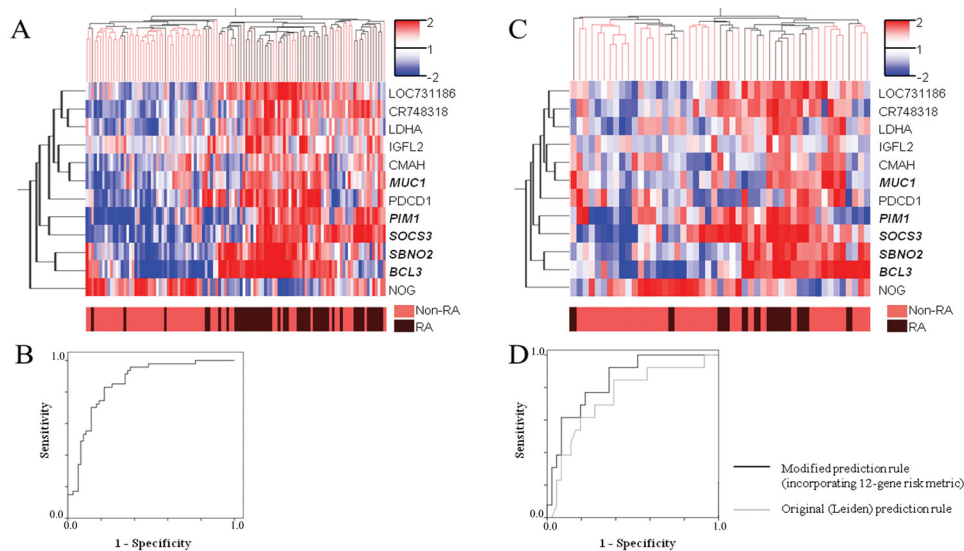


Figure 1 (A) Hierarchical clustering of training set: 111 samples represented by columns, and indicated individual genes by rows (italicised genes are STAT3 targets). Colour at each co-ordinate indicates gene-wise fold-expression relative to median (colour scale upper right). Underlying colour bar labels samples by inception diagnosis. (B) Receiver operator characteristic (ROC) plot for a rheumatoid arthritis (RA) risk metric derived from normalised gene expression values in the training cohort. Area under curve=0.85; SEM=0.04; $p < 0.001$. (C) Hierarchical clustering of anti-citrullinated peptide antibodies-negative undifferentiated arthritis 'validation' sub-cohort samples based on expression patterns of the same genes (interpretation as for figure 1A). (D) ROC curves comparing discriminatory value, in anti-citrullinated peptide antibodies-negative undifferentiated arthritis, of Leiden prediction rule (grey line) with a modified metric incorporating the 12-gene signature. Modified metric confers added value: area under ROC curve (original Leiden prediction rule)=0.74; SEM=0.08 versus area under ROC curve (modified metric incorporating gene signature)=0.84; SEM=0.06; $p < 0.001$ in both cases.

S2). Three lists of differentially expressed genes were then generated by comparing each of the 'inflammatory' groups (which themselves exhibited comparable acute phase responses) with the OA group (>1.2-fold change; uncorrected $p < 0.05$; online supplementary gene-lists 2–4). The three lists were overlapped on a Venn diagram (figure 2).

A highly significant over-representation of genes involved in the cell cycle was identified in association with ACPA-positive RA (24/43; $p < 1.0 \times 10^{-5}$); figure 2; online supplementary gene-list 5). In addition, genes involved in the regulation of apoptosis were over-represented in ACPA-negative RA patients, and RA was, in general, characterised by genes with functional roles in T cell differentiation (figure 2 online supplementary gene-lists 5–8). Importantly, within the highly significant 12-gene RA 'signature,' several genes (PIM1, SOCS3, SBNO2, BCL3 and MUC1) were noted to be STAT3-inducible based on literature sources.^{20–25} The majority of these were more markedly differentially expressed in ACPA-negative than ACPA-positive RA (figures 3A,B and online supplementary figures S4A–C). Additional STAT3-inducible genes (MYC, IL2RA)^{20 26 27} exhibited similar expression patterns, and there was a trend for STAT3 to be upregulated in ACPA-negative compared with ACPA-positive RA (online supplementary figures S4D–F). Moreover, a reciprocal pattern of expression across outcome groups was observed for the dominant negative helix-loop-helix protein-encoding gene inhibitor of DNA-binding 3 (ID3) (online supplementary figure S4G), consistent with its putative regulatory role in STAT3 signalling.²⁸ MYC and ID3, although absent from the discriminatory RA signature under the stringent significance thresholds used, were however robustly differentially expressed between RA and non-RA patients within the training cohort (table 2). Finally, in relation to both the 12-gene signature and the extended list of genes exclusively deregulated in ACPA-negative RA (online supplementary gene list 6), overlap

with independently predicted STAT3-inducible gene sets (see online supplementary text and supplementary gene list 9) confirmed a preponderance of STAT3-inducible genes (hypergeometric p -values < 0.005 in both cases; see online supplementary text) – which was not seen for genes deregulated only in ACPA-positive RA ($p = 0.19$).

Serum IL-6 is highest in ACPA-negative RA and independently predicts CD4 STAT3-inducible gene expression

Since one classical mechanism of STAT3 phosphorylation is via gp130 co-receptor ligation,²⁹ we hypothesised that increased systemic levels of a key gp130 ligand and pro-inflammatory cytokine, IL-6, may be responsible for the STAT3-mediated transcriptional programme in early RA patients. Baseline serum IL-6 was measured in 131 of the 173 EAC patients which were subsequently grouped according to their ultimate diagnosis (ACPA-negative RA, ACPA-positive RA, non-RA inflammatory arthropathy or OA). IL-6 levels were low overall (generally < 100 pg/ml), but were highest in the ACPA-negative RA group (figure 3C). Indeed, unlike the generic marker of systemic inflammation C reactive protein (CRP), baseline IL-6 discriminated ACPA-negative RA from non-RA inflammatory arthritides (figures 3C,D). Furthermore, among individuals for whom paired and contemporaneous serum IL-6 and PB CD4 T-cell RNA samples were available, clear correlations between IL-6 and the normalised expression of STAT3-inducible genes were seen (figures 4A–D; also online supplementary figures S5A–D); for example, serum IL-6 measurements correlated with normalised SOCS3 expression: Pearson's $R = 0.57$, $p < 0.001$ (figure 4A). Multivariate analysis confirmed that IL-6, but not CRP or TNF α (which does not signal via STAT3), independently predicted PB CD4 T cell SOCS3 expression ($\beta = 0.53$; $p < 0.001$; see online

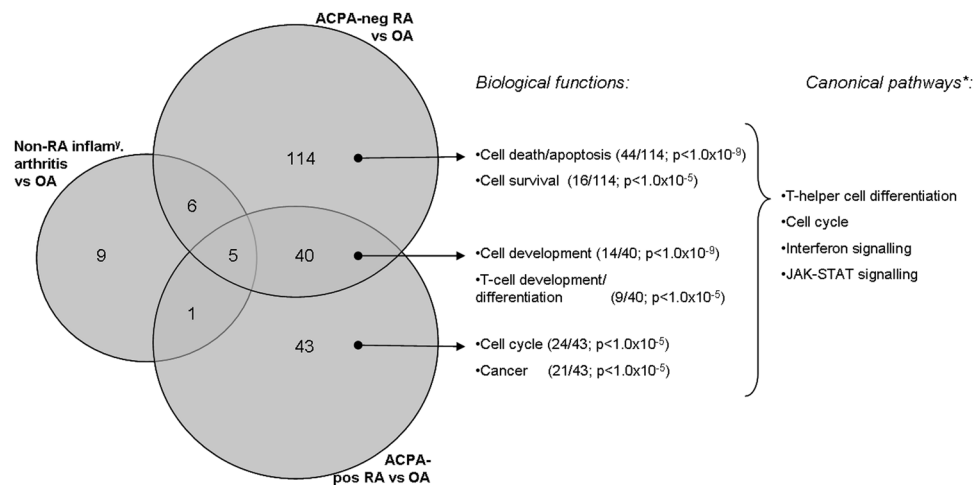


Figure 2 Functional analysis of array data. Genes differentially expressed (>1.2 -fold change; $p < 0.05$) between osteoarthritis (OA) and three separate inflammatory comparator groups were overlapped in a Venn diagram (see text, and online supplementary gene lists 2–4, for detailed list compositions). Genes uniquely deregulated in rheumatoid arthritis (RA) (anti-citrullinated peptide antibodies (ACPA)-negative, ACPA-positive or both) could thereby be identified and subjected to pathway analysis (see text). The top two over-represented biological functions identified for the three indicated sets are shown, along with the proportion of the set associated with the function in question, and a p value relating to the likelihood of given proportions occurring by chance (Fisher's exact test). Online supplementary gene lists 5–7 summarise functionally related genes thereby identified. The three indicated sets were combined to identify canonical pathways over-represented among genes differentially expressed between RA and OA in general. Pathways of particular interest in the biological context are listed (genes in question are listed in online supplementary gene list 8), *hypergeometric p-values (Fisher's exact) in each case < 0.01 .

supplementary table S6) excluding a more general influence of inflammation.

Given that only 30–50% of PB CD4 T cells are thought to express membrane-bound IL6R,³⁰ we also measured sIL6R (as a surrogate of IL-6R trans-signalling)³¹ and two other gp130 ligands, granulocyte colony stimulating factor and leptin, both of which have been implicated in RA pathogenesis.^{32–33} However, levels in sera from a subset of 80 study patients correlated with neither the diagnostic outcome nor the STAT3 gene expression. Finally, IL-10 and IL-17, which are both STAT3 activators,³⁴ were undetectable in the vast majority of sera (data not shown).

STAT3-inducible, RA-associated expression signature is activated by IL-6 in primary CD4 T cells of healthy donors in vitro

To confirm that the observed deregulated expression of STAT3 target genes among early RA patients was downstream of IL-6 signalling, primary human CD4 T cells were incubated in vitro with recombinant human IL-6 and the expression of relevant target genes measured at 1 and 6 h (see online supplementary text and figures S6–S7). Robust upregulation of SOCS3, PIM1, BCL3 and MYC was observed consistently 1 h after the addition of IL-6. A similar trend was seen for SBNO2, which became significant in the presence of recombinant soluble human IL-6 receptor. Conversely and consistent with prior observations, a distinct trend towards repression of ID3 was seen in response to IL-6 plus sIL6R.

DISCUSSION

We present a unique analysis of the CD4 T-cell transcriptome in a well-characterised inception cohort of early arthritis patients attending a routine EAC in UK. As a potential diagnostic tool, it is significant that our 12-gene 'RA expression signature' (table 2) performed best among the diagnostically challenging ACPA-negative UA patient group. Intriguingly, these findings

support the involvement of CD4 T cells in both ACPA positive and negative disease.

The signature's sensitivity and specificity (0.85 and 0.75) for predicting subsequent RA in seronegative UA patients equate to a positive likelihood ratio of 3.4, indicating that a prior probability of 25% for RA progression among this cohort (13 of the 49 patients progressed to RA) doubles to 53% for an individual who has been assigned a positive SVM classification.³⁵ Moreover, of the 13 ACPA-negative UA patients who progressed to RA in our cohort, 8 fell into an 'intermediate' risk category for RA progression according to the validated Leiden prediction score.⁵ Encouragingly, all but one of these patients were correctly classified based on their 12-gene expression profile. Our proposal that this approach might add value to existing algorithms for the diagnosis of ACPA-negative UA is further supported by the construction of ROC curves comparing the Leiden prediction rule with a modified risk metric that incorporates features of our gene signature (figure 1D).

Our data indicate that PB CD4 T cells in early RA are characterised by a predominant upregulation of biological pathways involved in cell cycle progression (ACPA-positive) and survival, death and apoptosis (ACPA-negative) (figure 2; also online supplementary gene lists 5–6). Pathway analysis also suggested that T-cell development and differentiation were deregulated in both RA serotypes (online supplementary gene list 7). These findings concur with previous observations of impaired T-cell homeostasis in RA, characterised by increased turnover, telomere shortening and immunosenescence.^{36–37} Given the well-characterised importance of the STAT3 signalling pathway in both oncogenesis and T-cell survival, it was notable that five genes from our statistically robust 12-gene RA signature are downstream of STAT3 signalling.^{20–25} The degree to which these genes sub-cluster according to the expression pattern among individuals in both the training and validation cohorts (figure 1A,C) presumably reflects their co-regulation by STAT3. Their upregulation was generally most pronounced in ACPA-negative RA (figure 3A,B; also online supplementary figure

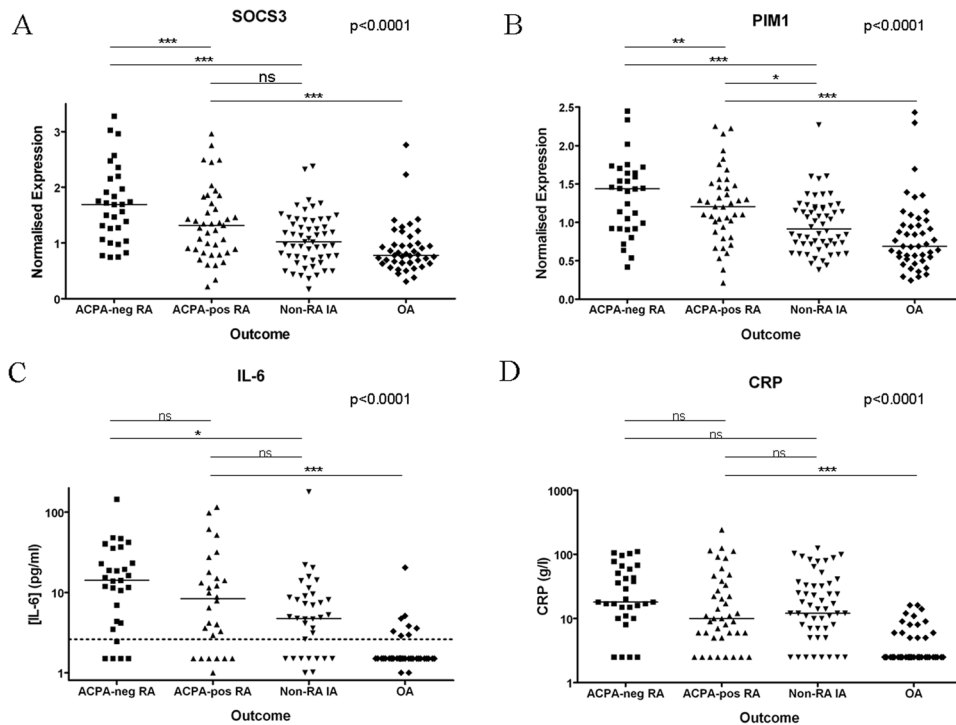


Figure 3 (A–B) Baseline profiles of indicated STAT3-regulated genes across four outcome groups; see online supplementary figure S4 and table S2 for additional examples and patient characteristics, respectively. (C–D) Baseline serum interleukin-6 (C; $n=131$) and C reactive protein (D; $n=173$) measurements across outcome groups. P-values: non-parametric analyses of variance (Kruskal–Wallis); for post-hoc analyses, 1, 2 and 3 asterisks denote $p<0.05$, 0.01 and 0.001, respectively (Dunn’s multiple comparison analysis). ACPA, anti-citrullinated peptide antibodies; IL-6, interleukin 6; NS, not significant; RA, rheumatoid arthritis; IA, inflammatory arthritis.

S4A–C), explaining why the predictive utility of the 12-gene signature was optimal in this disease subset.

Our observation that increased serum IL-6 levels among EAC attendees may predict a diagnosis of RA versus alternative arthritides is consistent with findings of previous biomarker studies,^{38–39} but ours is the first demonstration of a particular association with ACPA-negative disease (figure 3C). Striking correlations were seen between PB CD4 T-cell expression of several STAT3-inducible genes and paired, contemporaneous serum IL-6 concentrations, which were independent of alternative acute phase markers (figures 4A–D; also online supplementary figures S5A–D and table S6). STAT3 phosphorylation and downstream transcription is initiated by ligation of the cell-surface gp130 co-receptor by a range of ligands, including IL-6.⁴⁰ We measured IL-6 in particular because of its recognised role as a pro-inflammatory cytokine in RA,⁴¹ and we excluded similar relationships with sIL6R (a surrogate of IL-6R trans-signalling) and other relevant substrates of STAT3 signalling. Therefore, the STAT3-inducible gene expression signature that we have identified does appear to be downstream of IL-6 signalling. The capacity of IL-6 alone to induce the STAT-3-regulated elements of our early RA gene expression signature in primary CD4 T cells was confirmed in vitro (online supplementary figures S6 and S7).

In conclusion, our data provide strong evidence for the induction of an IL-6-mediated STAT3 transcription programme in PB CD4 T cells of early RA patients, which is most prominent in ACPA-negative individuals and which contributes to a gene expression ‘signature’ that may have diagnostic utility. Furthermore, our findings could pave the way for a novel treatment paradigm, whereby emerging drugs targeting the *IL-6-gp130-STAT3* ‘axis’^{42–43} find a rational niche as first choice agents in the management of ACPA-negative RA. Studies, such as ours,

should ultimately contribute to the realisation of true ‘personalised medicine’ in early inflammatory arthritis, in which complex heterogeneity is stratified into pathophysiologically and therapeutically relevant subsets, with clear benefits in terms of clinical outcome and cost.

Contributors AGP was involved in the study’s conception and design, sample and data collection; he conducted the majority of the laboratory work, performed a substantial part of the analysis and drafted the manuscript. DCS helped design the study and made a major contribution to data analysis, also contributing intellectually to revising the manuscript. SR made substantial contributions to the laboratory work, data analysis and manuscript revision. GW was involved in the study design and made a major contribution to the recruitment of patients, sample handling and the recording of clinical data, also critically appraising the manuscript draft. CH helped conceive and design the study, also contributing to the laboratory work and manuscript drafting. DAY helped conceive and design the study and performed some of the laboratory work; he also made a substantial contribution to data analysis, and contributed to manuscript drafting. JDI conceived and designed the study and contributed to data analysis; he provided intellectual input and supervision throughout the study and made a substantial contribution to manuscript drafting.

Acknowledgements AGP’s work was supported by a clinical research fellowship from the Arthritis Research Campaign, UK. This work was supported by the UK NIHR Biomedical Research Centre for Ageing and Age-Related Disease Award to the Newcastle upon Tyne Hospitals NHS Foundation Trust. Clinical and translational research in the Musculoskeletal Research Group is supported by the Northumberland, Tyne and Wear Comprehensive Local Research Network. The authors would like to thank the clinical staff at The Freeman Hospital who co-operated with the recruitment phase of the study, and, of course, the many patient volunteers who contributed so willingly.

Funding This study was supported by Arthritis Research UK (grant number 17983).

Competing interests None.

Ethics approval Ethics approval was provided by the Newcastle and North Tyneside Local Research Ethics Committee.

Provenance and peer review Not commissioned; externally peer reviewed.

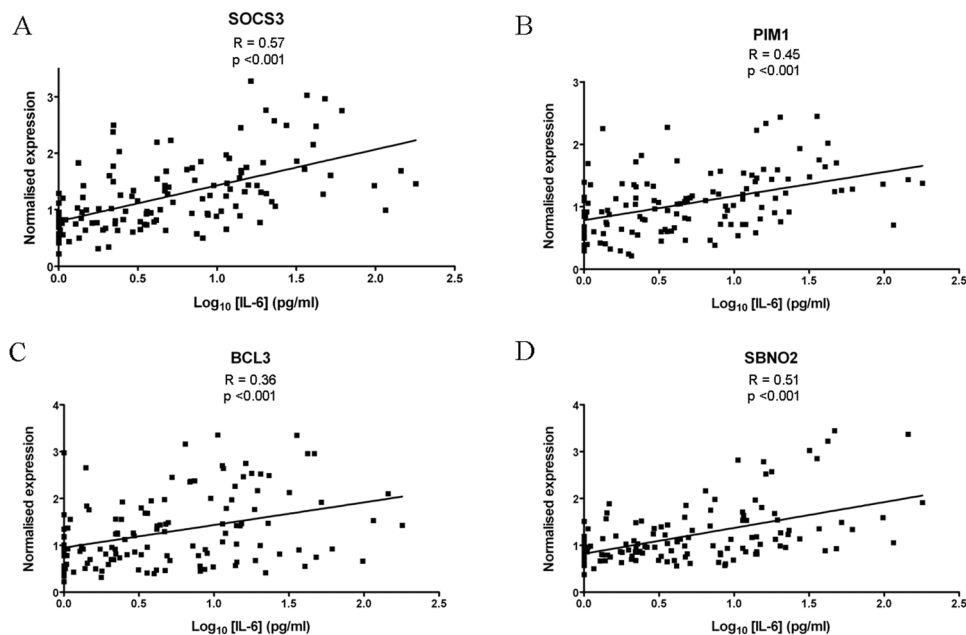


Figure 4 (A–D) Serum interleukin 6 (IL-6) concentrations correlate with STAT3-inducible gene expression in peripheral blood CD4 T cells (see online supplementary figure S5, for additional examples). Data are shown for 131 individuals in whom paired, contemporaneous samples were available at baseline; Pearson's R and associated p values are shown.

Data sharing statement Raw and processed microarray data used in this study is available via Gene Expression Omnibus at: <http://www.ncbi.nlm.nih.gov/geo/query/acc.cgi?token=bvfitkociimgsnk&acc=GSE20098>.

REFERENCES

- Klareskog L, Catrina AI, Paget S. Rheumatoid arthritis. *Lancet* 2009;**373**:659–72.
- Combe B, Landewe R, Lukas C, *et al*. EULAR recommendations for the management of early arthritis: report of a task force of the European Standing Committee for International Clinical Studies Including Therapeutics (ESCSIT). *Ann Rheum Dis* 2007;**66**:34–45.
- van Gaalen FA, Linn-Rasker SP, van Venrooij WJ, *et al*. Autoantibodies to cyclic citrullinated peptides predict progression to rheumatoid arthritis in patients with undifferentiated arthritis: a prospective cohort study. *Arthritis Rheum* 2004;**50**:709–15.
- Aletaha D, Neogi T, Silman AJ, *et al*. 2010 Rheumatoid arthritis classification criteria: an American College of Rheumatology/European League Against Rheumatism collaborative initiative. *Arthritis Rheum* 2010;**62**:2569–81.
- van der Helm-van Mil AH, Detert J, le Cessie S, *et al*. Validation of a prediction rule for disease outcome in patients with recent-onset undifferentiated arthritis: moving toward individualized treatment decision-making. *Arthritis Rheum* 2008;**58**:2241–7.
- Nishimura K, Sugiyama D, Kogata Y, *et al*. Meta-analysis: diagnostic accuracy of anti-cyclic citrullinated peptide antibody and rheumatoid factor for rheumatoid arthritis. *Ann Intern Med* 2007;**146**:797–808.
- Pratt AG, Isaacs JD, Wilson G. The clinical utility of a rule for predicting rheumatoid arthritis in patients with early undifferentiated arthritis: comment on the article by van der Helm-van Mil *et al*. *Arthritis Rheum* 2009;**60**:905; author reply 906.
- Pascual V, Chaussabel D, Banachereau J. A genomic approach to human autoimmune diseases. *Annu Rev Immunol* 2010;**28**:535–71.
- McKinney EF, Lyons PA, Carr EJ, *et al*. A CD8+ T cell transcription signature predicts prognosis in autoimmune disease. *Nat Med* 2010;**16**:586–91, 1p following 591.
- van Baarsen LG, Bos WH, Rustenburg F, *et al*. Gene expression profiling in autoantibody-positive patients with arthralgia predicts development of arthritis. *Arthritis Rheum* 2010;**62**:694–704.
- Batiwalla FM, Baechler EC, Xiao X, *et al*. Peripheral blood gene expression profiling in rheumatoid arthritis. *Genes Immun* 2005;**6**:388–97.
- Lyons PA, Koukoulaki M, Hatton A, *et al*. Microarray analysis of human leucocyte subsets: the advantages of positive selection and rapid purification. *BMC Genomics* 2007;**8**:64.
- McInnes IB, O'Dell JR. State-of-the-art: rheumatoid arthritis. *Ann Rheum Dis* 2010;**69**:1898–906.
- Arnett FC, Edworthy SM, Bloch DA, *et al*. The American Rheumatism Association 1987 revised criteria for the classification of rheumatoid arthritis. *Arthritis Rheum* 1988;**31**:315–24.
- Schroeder A, Mueller O, Stocker S, *et al*. The RIN: an RNA integrity number for assigning integrity values to RNA measurements. *BMC Mol Biol* 2006;**7**:3.
- Johnson WE, Li C, Rabinovic A. Adjusting batch effects in microarray expression data using empirical Bayes methods. *Biostatistics* 2007;**8**:118–27.
- Benjamini Y, Hochberg Y. Controlling the false discovery rate: a practical and powerful approach to multiple testing. *J R Stat Soc Series B Stat Methodol* 1995;**57**:289–300.
- Cortes C, Vapnik V. Support-vector networks. *Machine Learning* 1995;**20**:273–97.
- Livak KJ, Schmittgen TD. Analysis of relative gene expression data using real-time quantitative PCR and the 2(-Delta Delta C(T)) Method. *Methods* 2001;**25**:402–8.
- Owaki T, Asakawa M, Morishima N, *et al*. STAT3 is indispensable to IL-27-mediated cell proliferation but not to IL-27-induced Th1 differentiation and suppression of proinflammatory cytokine production. *J Immunol* 2008;**180**:2903–11.
- Starr R, Willson TA, Viney EM, *et al*. A family of cytokine-inducible inhibitors of signalling. *Nature* 1997;**387**:917–21.
- El Kasmi KC, Smith AM, Williams L, *et al*. Cutting edge: A transcriptional repressor and corepressor induced by the STAT3-regulated anti-inflammatory signaling pathway. (erratum appears in *J Immunol* 2008;180:3612 Note: Panopoulos, Athanasia (corrected to Panopoulos, Athanasia DJ)). *J Immunol* 2007;**179**:7215–9.
- Brocke-Heidrich K, Ge B, Cvijic H, *et al*. BCL3 is induced by IL-6 via Stat3 binding to intronic enhancer HS4 and represses its own transcription. *Oncogene* 2006;**25**:7297–304.
- Richard M, Louahed J, Demoulin JB, *et al*. Interleukin-9 regulates NF-kappaB activity through BCL3 gene induction. *Blood* 1999;**93**:4318–27.
- Gao J, McConnell MJ, Yu B, *et al*. MUC1 is a downstream target of STAT3 and regulates lung cancer cell survival and invasion. *Int J Oncol* 2009;**35**:337–45.
- Akaishi H, Takeda K, Kaisho T, *et al*. Defective IL-2-mediated IL-2 receptor alpha chain expression in Stat3-deficient T lymphocytes. *Int Immunol* 1998;**10**:1747–51.
- Matikainen S, Sareneva T, Ronni T, *et al*. Interferon-alpha activates multiple STAT proteins and upregulates proliferation-associated IL-2Ralpha, c-myc, and pim-1 genes in human T cells. *Blood* 1999;**93**:1980–91.
- Nichane M, Ren X, Bellefroid EJ. Self-regulation of Stat3 activity coordinates cell-cycle progression and neural crest specification. *EMBO J* 2010;**29**:55–67.
- Hirano T, Ishihara K, Hibi M. Roles of STAT3 in mediating the cell growth, differentiation and survival signals relayed through the IL-6 family of cytokine receptors. *Oncogene* 2000;**19**:2548–56.
- Nowell MA, Williams AS, Carty SA, *et al*. Therapeutic targeting of IL-6 trans signaling counteracts STAT3 control of experimental inflammatory arthritis. *J Immunol* 2009;**182**:613–22.
- Rose-John S, Scheller J, Elson G, *et al*. Interleukin-6 biology is coordinated by membrane-bound and soluble receptors: role in inflammation and cancer. *J Leukoc Biol* 2006;**80**:227–36.
- Eyles JL, Hickey MJ, Norman MU, *et al*. A key role for G-CSF-induced neutrophil production and trafficking during inflammatory arthritis. *Blood* 2008;**112**:5193–201.

33. **Rho YH**, Solus J, Sokka T, *et al.* Adipocytokines are associated with radiographic joint damage in rheumatoid arthritis. *Arthritis Rheum* 2009;**60**:1906–14.
34. **El Kasmí KC**, Smith AM, Williams L *et al.* Cutting edge: A transcriptional repressor and corepressor induced by the STAT3-regulated anti-inflammatory signaling pathway. (Erratum appears in *J Immunol* 2008;**180**:3612 Note: Panopoulos, Athanasia (corrected to Panopoulos, Athanasia D)). *J Immunol* 2007;**179**:7215–9.
35. **Altman DG**, Bland JM. Diagnostic tests 2: Predictive values. *BMJ* 1994;**309**:102.
36. **Ponchel F**, Morgan AW, Bingham SJ, *et al.* Dysregulated lymphocyte proliferation and differentiation in patients with rheumatoid arthritis. *Blood* 2002;**100**:4550–6.
37. **Goronzy JJ**, Weyand CM. Rheumatoid arthritis. *Immunol Rev* 2005;**204**:55–73.
38. **Kokkonen H**, Söderström I, Rocklöv J, *et al.* Up-regulation of cytokines and chemokines predates the onset of rheumatoid arthritis. *Arthritis Rheum* 2010;**62**:383–91.
39. **Karlson EW**, Chibnik LB, Tworoger SS, *et al.* Biomarkers of inflammation and development of rheumatoid arthritis in women from two prospective cohort studies. *Arthritis Rheum* 2009;**60**:641–52.
40. **Schindler CW**. Series introduction. JAK-STAT signaling in human disease. *J Clin Invest* 2002;**109**:1133–7.
41. **Fonseca JE**, Santos MJ, Canhão H, *et al.* Interleukin-6 as a key player in systemic inflammation and joint destruction. *Autoimmun Rev* 2009;**8**:538–42.
42. **Nishimoto N**, Miyasaka N, Yamamoto K, *et al.* Long-term safety and efficacy of tocilizumab, an anti-IL-6 receptor monoclonal antibody, in monotherapy, in patients with rheumatoid arthritis (the STREAM study): evidence of safety and efficacy in a 5-year extension study. *Ann Rheum Dis* 2009;**68**:1580–4.
43. **Cohen S**, Fleischmann R. Kinase inhibitors: a new approach to rheumatoid arthritis treatment. *Curr Opin Rheumatol* 2010;**22**:330–5.

Supplementary Methods.

Additional detail is provided under the same headings used in the main article. Where numbered references are not included in the main article, the full citation is given in parentheses in the text.

Patients.

An initial working diagnosis was assigned to each patient according to a “working diagnosis proforma” (*Table S1*). RA was diagnosed only where 1987 ACR classification criteria(14) were fulfilled; UA was defined as a “suspected inflammatory arthritis where RA remained a possibility, but where established classification criteria for any rheumatological condition remained unmet”. This working diagnosis was updated by the consulting rheumatologist at each subsequent clinic visit for the duration of the study – a median of 28 months and greater than 12 months in all cases.

CD4+ T-cell RNA processing and array analysis.

CD4+ T-cell RNA processing. Monocytes were first depleted by immunorsetting (Rosettesep[®] Human Monocyte depletion cocktail, Stemcell Technologies Inc., Vancouver, Canada), and remaining cells underwent positive selection using Easisep[®] whole blood CD4+ positive selection kit reagents in conjunction with the Robosep[®] automated cell separator (Stemcell). To confirm high CD4+ T-cell purity of isolates, flow cytometric analysis was completed for 148/173 (86%) of samples, and a median CD4+ CD14- purity of 98.9% was achieved (range 95 – 99.7%), with minimal CD4+ CD14+ monocyte contamination (median 0.32%; range 0.01 – 2.98%). Pilot work had demonstrated that incorporation of the monocyte depletion step described was

required to achieve this (*Figure S1A and B*). RNA was immediately extracted from CD4+ T-cell isolates using RNeasy MINI kits® (Qiagen GmbH, Germany), incorporating the manufacturer's recommended "on-column" DNA digestion step.

Microarrays. Microarray experiments were performed in 2 phases (phase I, 95 samples; phase II, 78 samples). In each case, total RNA quality was assessed using an Agilent 2100 Bioanalyzer (Agilent Technologies, Palo Alto, CA) according to standard protocols. 250ng RNA was reverse transcribed into cRNA, and biotin-UTP labeled, using the Illumina TotalPrep RNA Amplification Kit (Ambion, Texas). cRNA was hybridised to the Illumina Whole Genome 6 (version 3) BeadChip® (Illumina, San Diego, CA), following the manufacturer's protocol. Each BeadChip measured the expression of 48,804 genes (annotation file at http://www.illumina.com/support/annotation_files.ilmn) and was imaged using a BeadArray Reader (Illumina).

Bioinformatics: normalisation, batch-correction, filtering and quality control. Raw microarray data were imported into GeneSpring GX 7.3.1 software (Agilent Technologies), with which all statistical analyses were performed except where indicated. Phases I and II of the study were independently normalised in 2 steps: each probe measurement was first divided by the 50th percentile of all measurements in its array, before being centred around its own median expression measurement across all samples in the phase. The anticipated batch-effect noted between phases on their combination, in addition to minor within-phase batch effects relating to one of the Illumina TotalPrep RNA Amplification steps, was corrected in the R statistical computing environment (<http://www.r-project.org/>) using the empirical Bayes method

of Johnson *et al*(16). Raw and transformed data are available for review purposes at the Gene Expression Omnibus (GEO) address:

<http://www.ncbi.nlm.nih.gov/geo/query/acc.cgi?token=bviftkociimgsnk&acc=GSE20098>.

Genes detectably expressed (detection p-value <0.01) in ≥ 1 sample of each study phase passed filtering of the normalised and batch-corrected data, and were included in subsequent analyses (16,205 genes) [Du P, Kibbe WA, Lin SM. *lumi: a pipeline for processing Illumina microarray. Bioinformatics 2008;24(13):1547-8*]. After normalisation of the raw data and filtering of expressed genes, technical bias relating to processing batches was shown to have been successfully eliminated using the method of Johnson *et al* (*Figure S2*)(16).

In addition to pathway analysis using Ingenuity Pathways Analysis software (Ingenuity Systems, Redwood City, CA), an objectively derived list of STAT3-inducible genes was created for additional hypergeometric statistical testing by combining lists from two publically available databases (full list and web links given in *Supplementary Gene List 9*). Hypergeometric testing in this case was performed using Stat Trek on-line resource (<http://stattrek.com>).

Serum cytokine measurement. During baseline clinical assessment, between 1300hrs and 1630hrs, serum was separated and frozen at -80°C , undergoing a single freeze-thaw cycle before use. The highly sensitive electro-chemoluminescence detection system (Meso Scale Discovery [MSD], Gaithersberg, Maryland) was used for cytokine measurement, according to the manufacturer's instructions. The potential for heterophilic rheumatoid factors (RFs) in sera to cross-link capture and detection antibodies and contribute to spurious read-outs [de Jager W, Prakken BJ, Bijlsma JWJ

et al. Improved multiplex immunoassay performance in human plasma and synovial fluid following removal of interfering heterophilic antibodies. Journal of Immunological Methods 2005;300(1-2):124-35, Hueber W, Tomooka BH, Zhao X et al. Proteomic analysis of secreted proteins in early rheumatoid arthritis: anti-citrulline autoreactivity is associated with up regulation of proinflammatory cytokines. Annals of the Rheumatic Diseases 2007;66(6):712-9] was investigated in pilot work to this study. We first confirmed that a commercially available, proprietary cocktail of non-human sera (Heteroblock, Omega Biologicals Inc., Boseman, Montana) could successfully neutralise the demonstrable heterophilic activity of native RF in human serum. A known final concentration of recombinant interferon-gamma (IFN- γ) was “spiked” into the sample and, by comparing the calculated difference in standard sandwich ELISA readout (BD Pharmingen, New Jersey, USA) between spiked and un-spiked samples with the actual spiked IFN- γ concentration, the extent of heterophilic activity could be ascertained, and the neutralising effect of varying concentrations of Heteroblock determined (*Figure S3A*) [*de Jager W, Prakken BJ, Bijlsma JWJ et al. Improved multiplex immunoassay performance in human plasma and synovial fluid following removal of interfering heterophilic antibodies. Journal of Immunological Methods 2005;300(1-2):124-35*]. We next measured IL-6 concentration in 24 RF+ serum samples (median RF by nephelometry = 165 IU) and 56 RF-negative samples, using the MSD platform, in each case running parallel assays with and without an optimised final concentration of Heteroblock. For the RF+ samples, excellent correlation was seen between assays performed with and without heteroblock (intraclass correlation coefficient = 0.98 [95% CI=0.95-0.99]). A Bland-Altman plot confirmed that any such discrepancy that did exist was no less evident in RF-negative samples, suggesting that interference by heterophilic RFs in sera

analysed using this platform is inconsequential (*Figure S3B*). All serum measurements reported in the current study were therefore carried out using the MSD platform in the absence of Heteroblock.

Derivation of risk metrics for ACPA-negative UA. Leiden prediction scores were calculated for each member of the training cohort according to baseline clinical and laboratory data as described in *Reference 5, main article*. Risk metrics based on the 12-gene RA "signature" were the sum of normalised expression values for all the genes therein, with the important exception of NOG (down-regulated in RA) whose normalised expression was instead subtracted. This latter modification ensured that the tendency for component genes to be up- or down-regulated in RA versus non-RA in the training cohort was accounted for in the derivation. Hence, in an individual example where 11/12 genes (all except NOG) were up-regulated relative to their median expression across all samples, each having a normalised expression of "+1" (sum = +11), but where NOG was down-regulated (normalised expression "-1"), the resultant risk metric would be "(+11 -[-1]) = +12, denoting a high risk of progression to RA.

Within the training dataset, both the Leiden prediction score and the 12-gene risk metric were entered as independent continuous variables into a logistic regression analysis with RA *versus* non-RA outcomes as the dependent variable (*Table S4*). In the resultant model the probability of an outcome of RA is related to both variables via the *modified* metric: $B_1x_1+B_2x_2$, where B_1 and B_2 are the regression coefficients for the Leiden prediction score and 12-gene risk metric respectively (B values in *Table S4*), and x_1 and x_2 are the values for each amongst individual patients. Hence,

for a given patient the modified metric is equal to: $(0.98 \times [\text{Leiden prediction score}]) + (0.36 \times [12\text{-gene risk metric}])$.

In vitro STAT3-inducible gene induction. To confirm that the observed deregulated expression of STAT3 target genes amongst early RA patients was a particular downstream feature of IL-6 signalling, primary human CD4⁺ T-cells were incubated *in vitro* with recombinant human IL-6, and expression of relevant target genes measured at 1 and 6 hours. Peripheral whole blood from 5 healthy volunteers underwent monocyte depletion and positive selection of CD4⁺ T-cells as described for patient volunteers, triplicate well experiments then being carried out for each donor. Cells were resuspended in serum-free RPMI + L-glutamine at a density of 1 million cells/ml and incubated (37°C, 5% CO₂) in the presence of media alone, recombinant human IL-6 (50ng/ml), or IL-6 (50 ng/ml) and an equimolar concentration of recombinant human sIL-6R (both Peprotech Inc., New Jersey, USA). At baseline, 1 and 6 hours, cells underwent immediate lysis and RNA extraction using RNeasy MICRO-*plus* kits® (Qiagen GmbH, Germany) according to the manufacturer's instructions. For TaqMan PCR assays in these experiments, 20ul reactions each incorporated 2.5ng cDNA, 10ul TaqMan Gene Expression Mastermix (Applied Biosystems), 0.4pmol each of forward and reverse primers designed using the on-line Universal ProbeLibrary facility (Roche Diagnostics, UK; <http://www.roche-applied-science.com>) and 0.2pmol of appropriate FAM-labelled ProbeLibrary probe, as summarised for each gene of interest in *Table S7*. 18S reactions differed, incorporating 0.4pmol each and 0.2pmol of primers and probe respectively (see *Table S7*), and 0.5ng cDNA. Cycling conditions for all reactions were as described

(Litherland GJ et al. Journal of Biological Chemistry 2008;283(21):14221-9). Raw data were normalized and expressed relative to 18S.

The results of these experiments are shown in online supplementary Figure S6.

Robust up-regulation of SOCS3, PIM1, BCL3 and MYC was observed consistently 1 hour after the addition of IL-6. A similar trend was seen for SBNO2, which became significant in the presence of recombinant soluble human IL-6 receptor. Conversely, and consistent with prior observations, a distinct trend towards repression of ID3 was seen in response to IL-6 plus sIL-6R, although this only reached significance at 6 hours. **Notably, there was inter-individual variability in the dynamics of ID3 repression, accounting for loss of significance when data were pooled (see *online supplementary Figure S7*).**

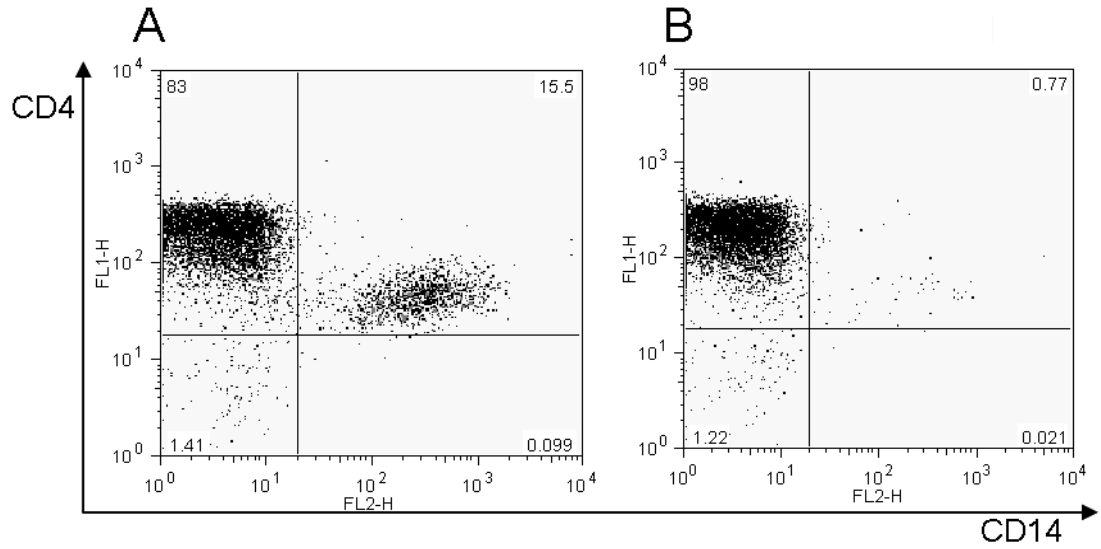


Figure S1: Flow cytometric analysis of CD4⁺ positive-selection isolate before (A) and after (B) the monocyte-depletion step described in *Methods*. The extent of CD4⁺ CD14⁺ monocyte contamination varies, but may be as high as 15%, as in this example.

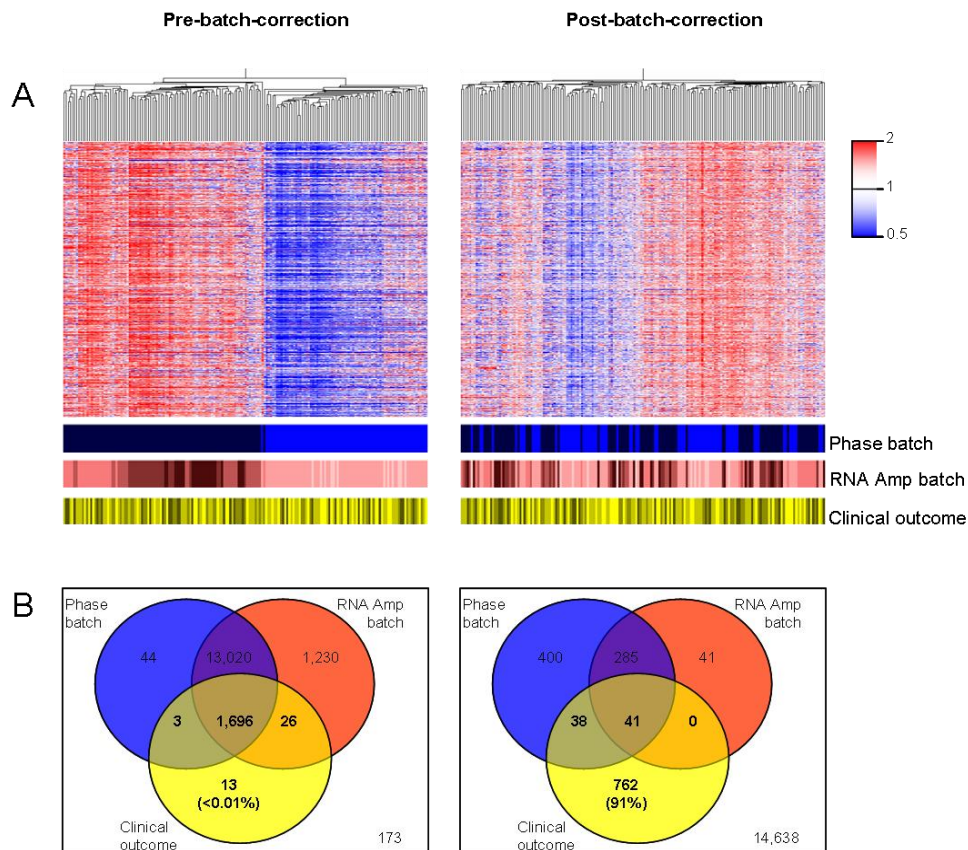
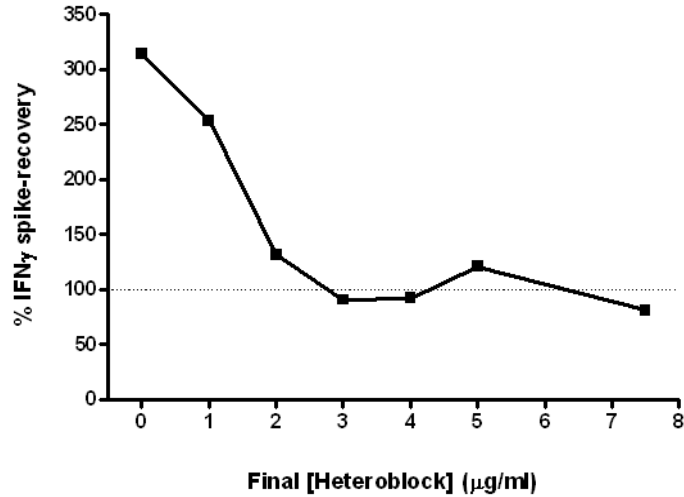


Figure S2. Outputs for normalised expression data of 16,205 genes that passed filtering is shown amongst 173 samples before and after batch-correction using the method of Johnston et al (left and right panels respectively) (reference 16). **A.** Unsupervised hierarchical clustering of samples based on correlations in gene expression patterns (standard correlation, average linkage, represented by dendrogram). 173 samples are represented by columns and individual genes by rows; the colour at each co-ordinate indicates gene-wise fold-expression relative to median, according to the colour scale to the right of the figure. Underlying blue, red and yellow colour-bars label samples according to membership of phase batch (n=2), RNA amplification batch (n=6) and the clinical outcome category of interest (n=4; ACPA-negative RA, ACPA-positive RA, inflammatory or non-inflammatory controls). Artefactual clustering according to technical parameters (phase of study or within-phase RNA amplification batch) is eliminated through batch-correction, which does not of itself unmask clustering based on the clinical outcome of interest. **B.** Lists of genes that varied significantly ($p < 0.05$ ANOVA) according to a sample's membership of phase batch (blue), RNA amplification batch (red) or clinical outcome of interest (yellow). Categories were generated amongst 16,205 passed genes, and overlapped in a Venn diagram. Without batch-correction virtually all genes seen to associate with clinical outcome are co-influenced by technical parameters. This potential source of technical bias is eliminated in 91% of outcome-related genes by the process of batch-correction. All genes named and discussed in this manuscript fell within this 91%.

A



B

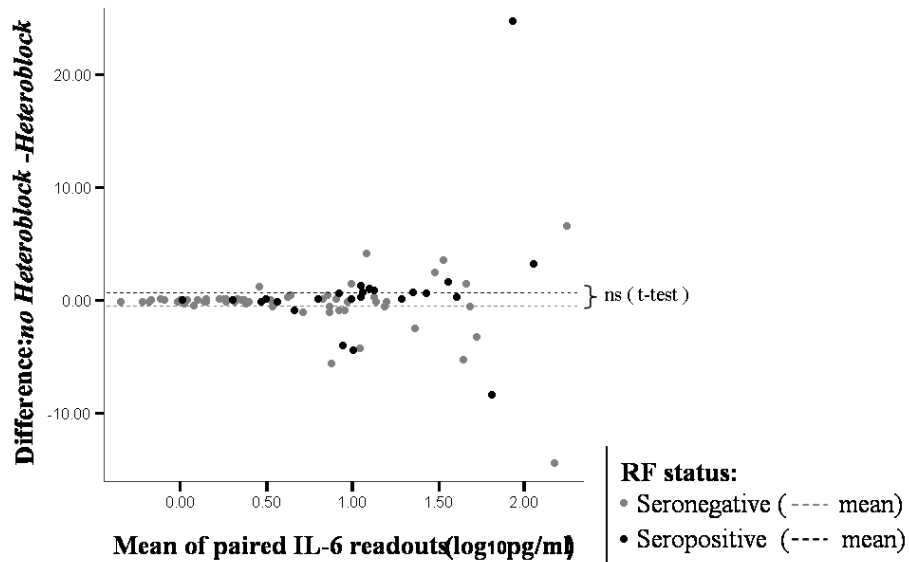


Figure S3. **A.** Titration of proprietary cocktail of non-human sera (*Heteroblock*; see text) against IFN- γ spike recovery in exemplar RF+ human serum sample. In the absence of Heteroblock the difference in read-out between spiked and un-spiked samples (“spike recovery”) is significantly greater than the known spiked IFN- γ amount ($>100\%$), indicating spuriously high assay readout due to the presence of heterophilic RF. Addition of $\geq 3\text{mg/ml}$ final concentration of Heteroblock neutralises this heterophilic effect. **B.** Bland-Altman plot of IL-6 readouts for 24 RF+ and 56 RF- serum samples obtained using MSD electrochemoluminescence platform, comparing assays performed in the presence / absence of a $3\mu\text{g/ml}$ final [Heteroblock]. No significant discrepancy is seen between RF+ and RF- samples in respect of the mean readout difference of the 2 assays. This indicates that the presence of potentially heterophilic antibodies is unlikely to affect assay readout in this system.

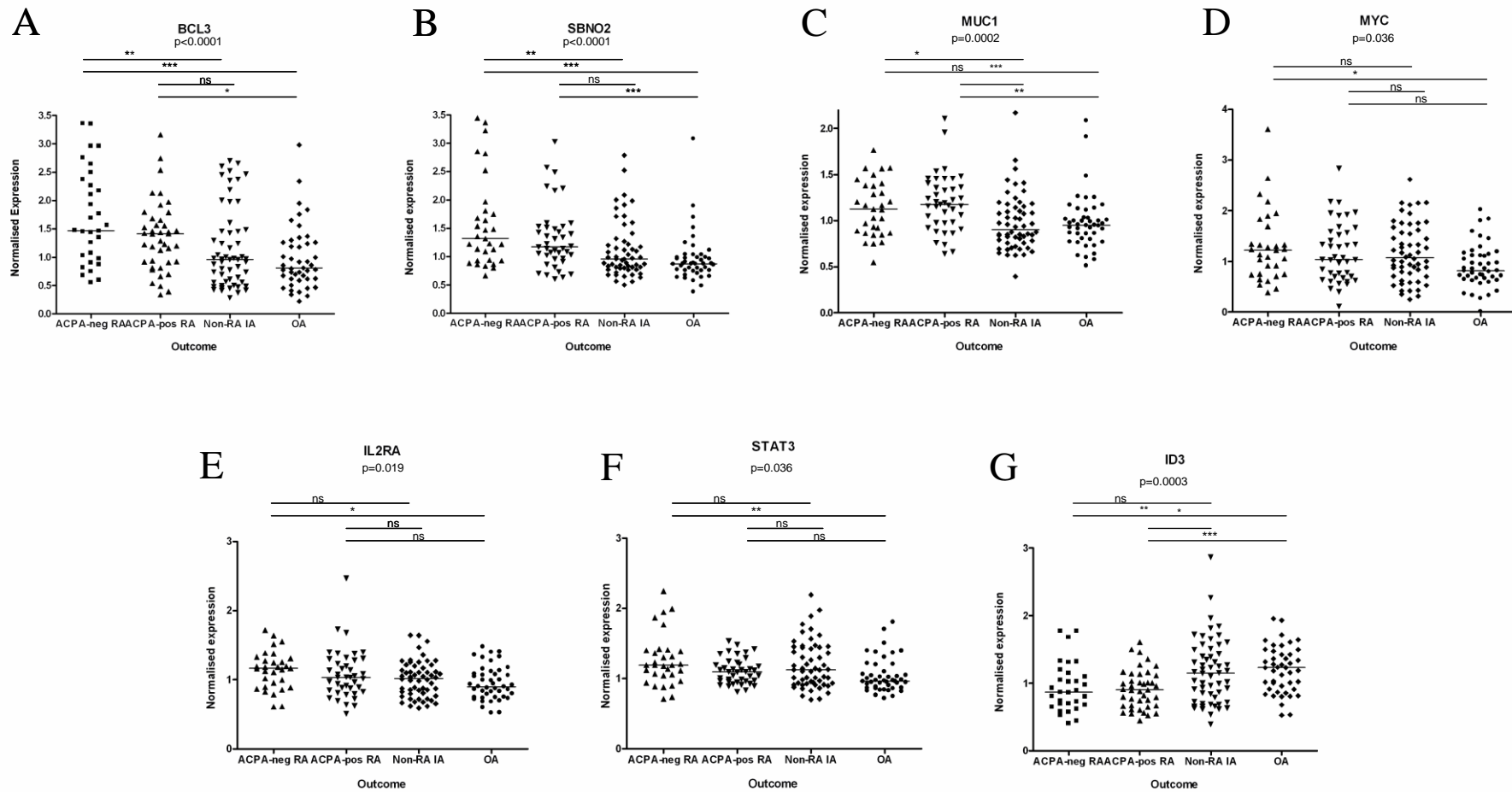


Figure S4. PB CD4⁺ T-cell expression profiles of indicated genes across 4 comparator groups, continued from *Figure 3*; see *Table S4* for characteristics of comparator groups. P-values shown are derived from non-parametric analysis of variance (Kruskal-Wallis); for *post-hoc* analyses, 1, 2 and 3 asterisks denote p < 0.05, 0.01 and 0.001 respectively (Dunn's multiple comparison analysis).

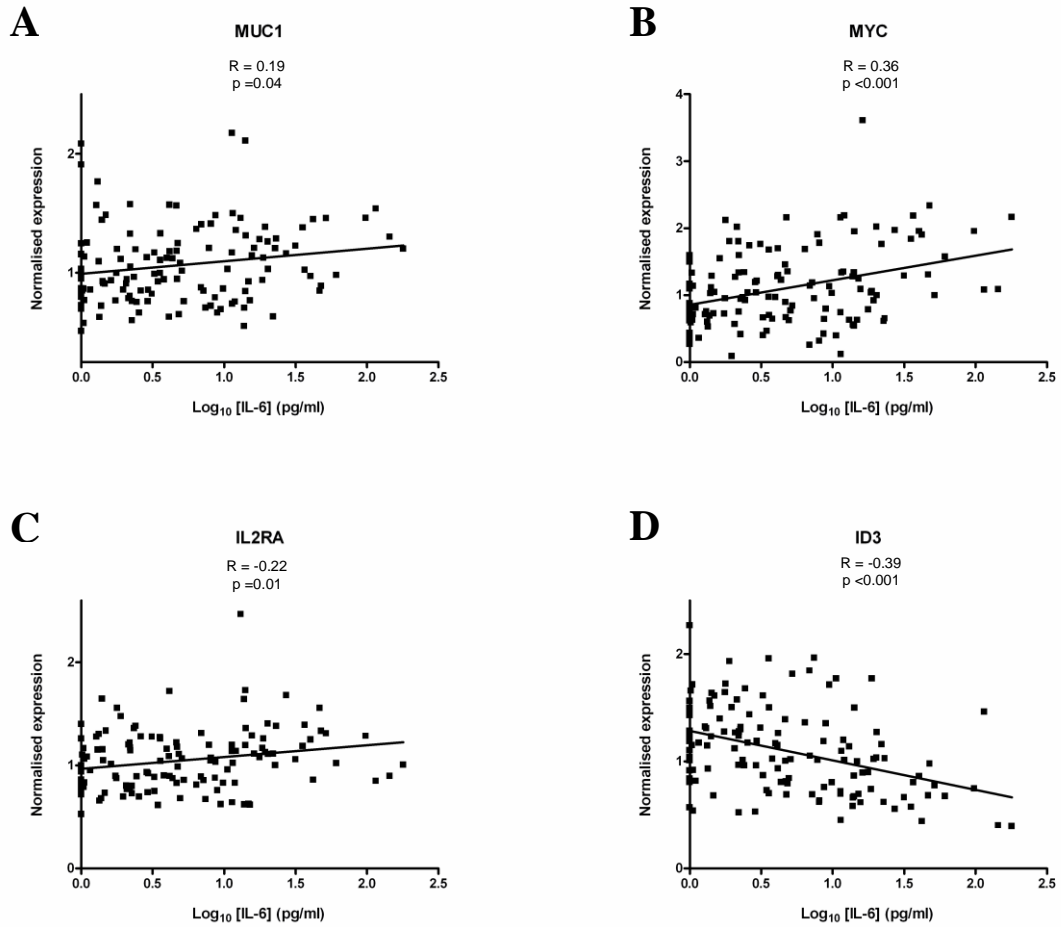


Figure S5. Serum IL-6 concentrations correlate with STAT3-inducible gene expression in PB CD4⁺ T-cells, continued from *Figure 4*. Data are shown for 131 individuals in whom paired, contemporaneous samples were available; Pearson's R and associated p-values are shown.

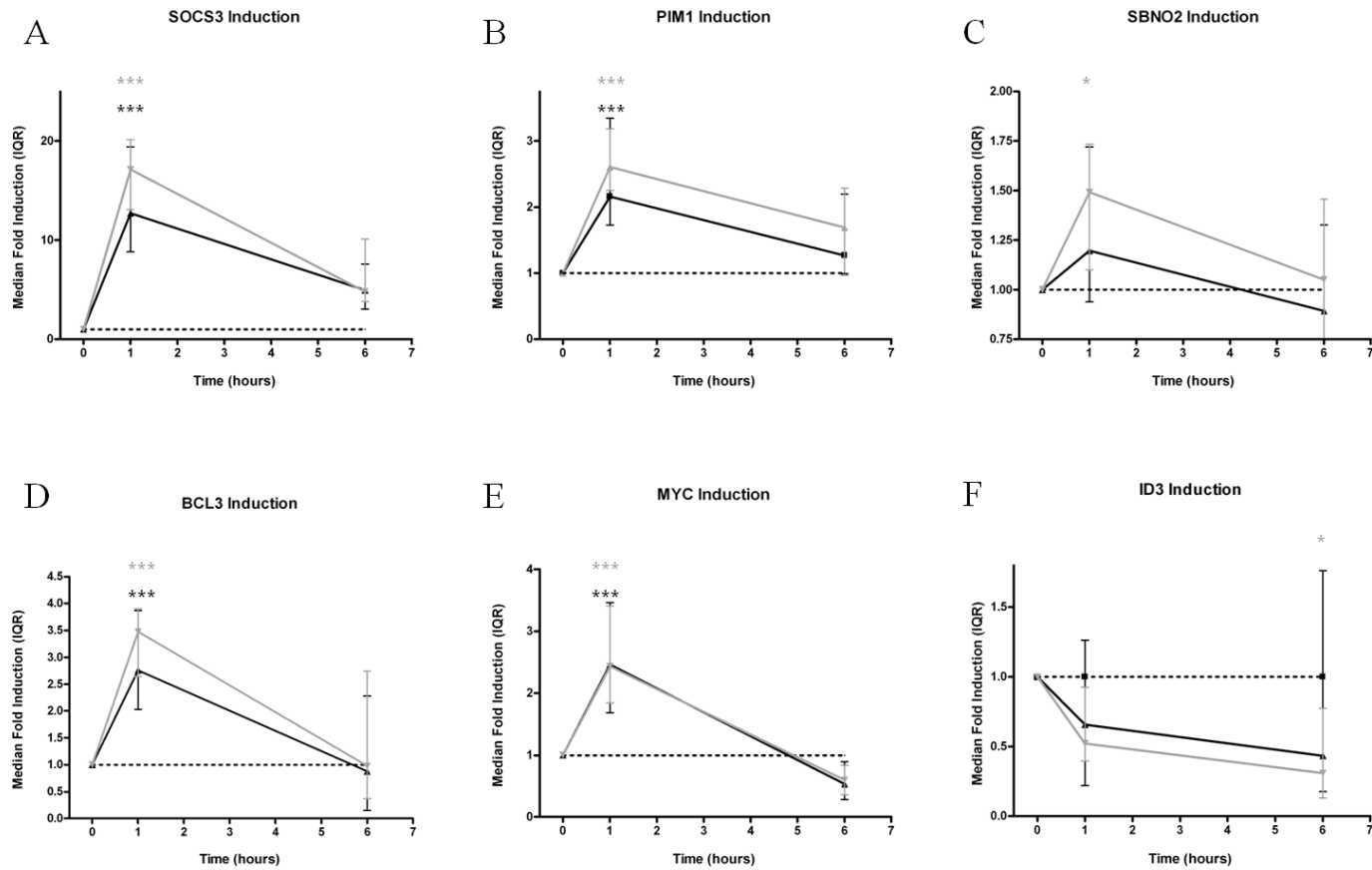


Figure S6. A-F. IL-6 regulates gene expression in CD4⁺ T-cells in viro. Purified CD4⁺ T-cells were incubated in the presence of IL-6 (black lines), IL-6 + sIL-6R (grey lines) or media alone (serum-free RPMI; dotted lines). Experiments carried out in triplicate; pooled data from 5 healthy donors is shown, scaled relative to media alone. 1, 2 and 3 asterisks denote $p < 0.05$, 0.01 and 0.001 respectively. (MWU test).

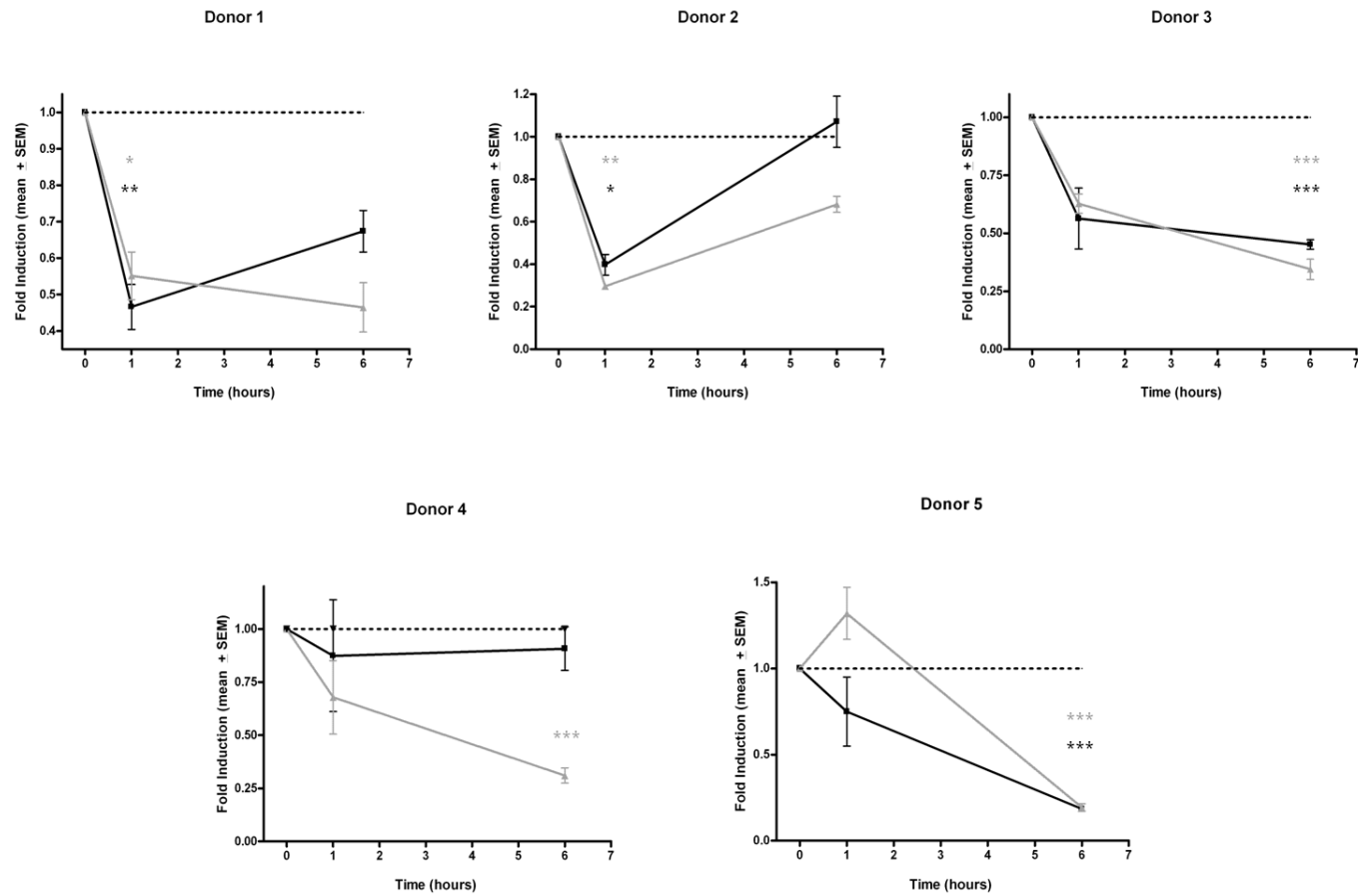


Figure S7. Repression of ID3 gene expression in CD4⁺ T-cells of 5 individual healthy donors, demonstrating heterogeneity of response. Purified CD4⁺ T-cells were incubated at 37°C for 1 or 6 hours in the presence of IL-6 (black lines), IL-6 + sIL-6R (grey lines) or media alone (RPMI; dotted lines). Experiments carried out in triplicate; pooled data from 5 healthy donors is shown, scaled relative to media alone. 1, 2 and 3 asterisks denote $p < 0.05$, 0.01 and 0.001 respectively (MWU test).

• RA		<input type="checkbox"/>	
• UA		<input type="checkbox"/>	
• Non-RA: “Inflammatory”	Psoriatic arthritis	<input type="checkbox"/>	
	Reactive /self-limiting inflammatory arthritis	<input type="checkbox"/>	
	Ankylosing spondylitis*	<input type="checkbox"/>	
	Enteropathic arthritis	<input type="checkbox"/>	
	Undifferentiated spondyloarthritis (not RA)	<input type="checkbox"/>	
	CTD	<input type="checkbox"/>	
	Crystal	<input type="checkbox"/>	
	Other	<input type="checkbox"/>	
	“Non-inflammatory”	Osteoarthritis	<input type="checkbox"/>
		Noninflammatory arthralgia / other.	<input type="checkbox"/>

Table S1. Categorisation of working diagnoses used amongst early arthritis patients at inception and follow-up during the course of this study. Consultant rheumatologists were asked to tick one box at each clinic visit, indicating the best description of their expert opinion of the diagnosis at a given time. See text. *Where modified New York criteria for the diagnosis of ankylosing spondylitis were not met, but the diagnosis was suspected in the context of seronegative inflammatory disease, consultants were asked to record a diagnosis of “undifferentiated spondyloarthritis”.

	ACPA- neg RA (n=31)	ACPA- pos RA (n=41)	Non-RA Inflam^y. (n=56)	Non-RA (OA / non-inflam^y.) (n=45)	p ^A (3xInflam ^y .)	p ^B (4xgroups)
Age (years; mean, SD)	61 (46-77)	56 (44-70)	44 (30-60)	52 (40-64)	<0001	<0.0001
% Female	66	61	62	80	NS	NS
Symptom durn. (wk; median, IQR)	12 (10-20)	12 (9-22)	12 (8-25)	32 (20-89)	NS	<0.0001
Tender joint count (median, IQR)	10.5 (5-15.5)	10 (3.5-16.5)	5 (2-13)	9 (2.5-19)	NS	NS
Swollen joint count (median, IQR)	4 (1-4)	3 (0.5-7.5)	1 (0-4)	0 (0-0.5)	<0.001	<0.0001
Morning stiffness (hrs; median, IQR)	1 (1-3.6)	1 (0.6-2.5)	1 (0.25-2)	0.5 (0.2-1.6)	NS	0.005
ESR (s; median, IQR)	48 (27-68)	54 (27-73)	34 (20-72)	20 (9.5-30)	NS	<0.0001
CRP (g/l; median, IQR)	18 (10-57)	10 (5-35)	13 (5-23)	2.5 (2.5-6)	NS	<0.0001
%ACPA+	0	100	0	2	<0.0001	<0.0001-
%RF+	25	93	11	12	<0.0001	<0.0001
DAS28 (median, IQR)	4.9 (4.5-5.9)	5.2 (4.1-6.0)	-	-	-	-

Table S2. Clinical characteristics of subjects as used in pathway analysis of pooled sample-set (n=173), divided into 4 comparator groups by outcome at >1 year follow-up: ACPA-negative RA, ACPA-positive RA, inflammatory and non-inflammatory control groups. Values are mean (1 SD range), median (IQR) or % for normally-distributed, skewed or dichotomous data respectively. ^Astatistical tests for significant variance between 3 inflammatory comparator groups (ACPA-negative RA, ACPA-positive RA and non-RA inflammatory arthritis); ANOVA, Kruskall-Wallis or Chi-square tests for normally-distributed, skewed or dichotomous data respectively. ^Bstatistical tests for significant variance between all 4 inflammatory comparator groups; ANOVA, Kruskall-Wallis or Chi square tests for normally-distributed, skewed or dichotomous data respectively; NS: not significant.

	Validation cohort		p ^A
	UA-RA (n=25)	UA-Non-RA (n=37)	
Age (years; mean, SD range)	58 (44-72)	48 (33-63)	0.01
% Female	72	81	NS
% White Caucasian	88	92	NS
Symptom duration (weeks; median, IQR)	12 (10-20)	20 (12-34)	NS
Tender joint count (median, IQR)	10 (5-16)	6 (2-17)	NS
Swollen joint count (median, IQR)	1 (0-4)	1 (0-1.5)	0.05
Morning stiffness (hours; median, IQR)	1.2 (0.75-4)	0.75 (0.4-2)	NS
ESR (s; median, IQR)	38 (22-59)	26 (18-60)	NS
CRP (g/l; median, IQR)	10 (2.5-20)	8 (2.5-15)	NS
ACPA+ (number; percentage)	12 (48%)	1 (3%)	<0.01
RF+ (number; percentage)	12 (48%)	8 (22%)	0.03
Leiden prediction score (median, IQR)	7.6 (6.8-8.5)	5.4 (4.4-6.7)	<0.01

Table S3. Demographic, clinical and serological characteristics of the UA-RA and UA-non-RA groups making up the validation patient cohort. Values are mean (1 SD range), median (IQR) or % for normally-distributed, skewed or dichotomous data respectively. ^AStatistical tests for significant difference between RA and Non-RA groups; t-test, Mann-Whitney U or Fisher's exact test for normally-distributed, skewed or dichotomous data respectively. CRP: C-reactive protein; RF: rheumatoid factor; NS: not significant.

	Training cohort		p ^A
	RA (n=32)	Non-RA (n=41)	
Age (years; mean, SD range)	58 (44-72)	45 (31-60)	<0.001
% Female	60	66	NS
% White Caucasian	94	89	NS
Symptom duration (weeks; median, IQR)	12 (9-23)	22 (12-52)	0.032
Tender joint count (median, IQR)	11 (5-19)	7 (4-17)	NS
Swollen joint count (median, IQR)	7 (1-11)	0 (0-3)	<0.001
Morning stiffness (hours; median, IQR)	1 (1-2)	1 (0.1-2)	0.024
ESR (s; median, IQR)	53 (30-79)	26 (15-57)	0.004
CRP (g/l; median, IQR)	17 (9-65)	5 (2.5-28)	0.007
ACPA+ (number, percentage)	22 (69%)	0 (0%)	<0.001
RF+ (number, percentage)	24 (75%)	2 (5%)	<0.001
DAS28 (median, IQR)	5.3 (4.2-6)	n/a	-
Outcome Diagnosis (number, percentage)			
RA	100 (100%)	0 (0%)	-
Seroneg Spond	-	14 (34%)	-
Self-limiting inflam.	-	7 (17%)	-
Other inflam.	-	2 (5%)	-
OA/non-inflam.	-	18 (44%)	-

Table S4. Clinical characteristics of the RA and non-RA comparator groups used in the training cohort subset amongst which TLDA validation was carried out (n=73/111). Values are mean (1 SD range), median (IQR) or % for normally-distributed, skewed or dichotomous data respectively. ^AStatistical tests for significant difference between RA and Non-RA groups; t-test, Mann-Whitney U or Fisher's exact test for normally-distributed, skewed or dichotomous data respectively. Seroneg. spond: seronegative spondyloarthritis; CRP: C-reactive protein; RF: rheumatoid factor; DAS28: disease activity score (incorporating 28- swollen / tender joint counts); NS: not significant

Variable	B	SE (B)	Wald	p-value	OR (95% CI)
12 gene risk metric	0.36	0.1	11.0	0.001	1.4 (1.2-1.8)
Leiden prediction rule	0.98	0.2	21.4	<0.001	2.5 (1.7-3.7)
Constant	-10.2	1.8	30.8	<0.001	-

Table S5. Results of logistic regression analysis for RA versus non-RA diagnoses amongst 111 EA patients in the training cohort. **B**: regression coefficients; **SE(B)**: standard error for B; **OR**: odds ratio; **CI**: confidence interval. The 12-gene risk metric for a given patient is the sum of normalised expression values for 12 genes in the putative RA signature (value for NOG subtracted; see text). The Leiden prediction rule is calculated according to reference (5). Both scores have independent predictive value in discriminating clinical outcomes of interest. Regression coefficients for each are used for the calculation of modified risk metrics amongst the independent cohort of ACPA-negative UA patients (see text).

Serum Variable	Unstandardised coefficients:		Standardised coefficients :	p-value	95% CI (B) (lower, upper)
	B	SE (B)	β		
Log ₁₀ [IL-6]	0.21	0.05	0.53	<0.001	0.12, 0.30
Log ₁₀ [CRP]	0.06	0.04	0.13	0.18	-0.03, 0.15
Log ₁₀ [TNFα]	-0.09	0.09	-0.08	0.32	-0.27, 0.09
Constant	-0.12	0.05	-	0.026	-0.23, -0.02

Table S6. Results of standard linear regression analysis to identify related serum variables independently associated with STAT-3 inducible gene expression amongst 131 EA clinic patients. The dependent variable was Log₁₀(normalised SOCS3 gene expression). SE (B): standard error for B; CI: confidence interval. All variables underwent prior transformation in order to satisfy normality conditions of standard linear regression. Only serum [IL-6] is independently associated with CD4+ T-cell SOCS3 expression (p<0.001; see text).

Gene	Forward Primer	Reverse Primer	Probe
(Accession N ^o .)			
18S (NR_003286)	cgaatggctcattaatcagttatgg	tattagctctagaattaccacagttatcc	tccttggctgctcgctcctc
SOCS3 (NM_003955)	agacttcgattcgggacca	aacttgctgtgggtgacca	UPL 36
PIM1 (NM_002648)	gatttccgactggggagag	agtccaggagcctaataatgacg	UPL 18
BCL3 (NM_005178)	cgacatctacaacaacctacgg	ccacagacggtaatgtggtg	UPL 39
MYC (NM_002467)	caccagcagcgactctga	gatccagactctgaccttttgc	UPL 34
SBNO2 (NM_014963)	aaagacctgcgactttgctc	ggacgaggagaagatggaga	UPL 63
ID3 (NM_002167)	catctccaacgacaaaaggag	ctccggcaggagaggtt	UPL 59

Table S7. Primers and probes used for real time PCR . UPL: *Universal ProbeLibrary*; numbers as designated on web-site referenced in Methods.